

ACTIVE WATER MANAGEMENT FOR PROTON EXCHANGE MEMBRANE FUEL CELLS USING AN INTEGRATED ELECTROSMOTIC PUMP

Cullen R. Buie*, Jonathan D. Posner, Tibor Fabian, Suk-Won Cha, Fritz B. Prinz, John K. Eaton, Juan G. Santiago
Department of Mechanical Engineering, Stanford University

ABSTRACT

We have developed proton exchange membrane fuel cells (PEMFC's) with integrated planar electroosmotic pumping structures that actively remove liquid water from cathode flow channels. Recent experimental and numerical investigations on PEMFC's emphasize water management as a critical factor in the design of robust, high efficiency fuel cells. Although various passive water management strategies have been proposed, water is still typically removed by pumping air into cathode channels at flow rates significantly larger than those required by fuel cell stoichiometry. This method of water removal is thermodynamically unfavorable and constrains cathode flow channel design. EO pumps can relieve cathode design barriers and simplify water management in fuel cells. EO pumps have no moving parts, scale across a wide range of operation, and result in low parasitic power. We demonstrate and quantify the efficacy of EO water pumping using a single-pass fuel cell test channel. Our results show that removing water from the cathode using integrated EO pumping structures improves fuel cell performance and stability. These pumps enable operation with air flow rates of just two to three times stoichiometric requirements.

INTRODUCTION

Proton exchange membrane fuel cells (PEMFCs) can potentially replace batteries in a wide range of hand-held electronics, and offer the possibility of large power densities and emission-free operation for cars [1,2]. Recent experimental and numerical studies on PEMFCs suggest that a critical factor in the design of high efficiency, robust systems is dealing with liquid water produced by the oxygen reduction reaction at the cathode [1,3,4,]. Water build-up in these systems decreases performance and inhibits robust operation [3-8]. Water management in PEMFCs can be divided into two general methodologies: passive and active. Passive water management involves designs where water is accumulated during operation or more efficiently removed without consuming additional power. An example is the incorporation of hydrophilic wicking structures into PEMFC cathode flow channels to redistribute liquid water [9]. Active water management schemes consume power and can be implemented intermittently in order to remove accumulated liquid water. Knobbe et al. proposed a method of active water management

that involves controlling the delivery of air to various cells in a PEMFC stack in order to purge water only from flooded cells [10,11]. As an alternative active water management scheme, we propose direct removal of liquid water from the cathode using electroosmotic pumping. Electroosmotic (EO) pumps have no moving parts and scale across a wide range of operation. With proper implementation, EO pumps can radically change designs by decreasing pump work delivered to air streams.

NOMENCLATURE

A	pump cross sectional area
a	pore radius
F	Faraday constant
I''_{eo}	EO pump current (per unit area)
j	current density
L	pump thickness
M	molecular weight
P''_{eo}	power consumed by EO pump (per unit area)
ΔP	pressure drop
Q	flowrate
R_A	resistance between electrode and EO pump
R_u	universal gas constant
s	volume fraction of oxygen in air
t	time
T	temperature
V_{FC}	fuel cell voltage
V_{eff}	effective potential drop across pump
V_{app}	applied potential drop across pump
V_{dec}	decomposition potential
α	ratio of actual air flow rate to stoichiometric flow rate
β	ratio of water flow rate to air flow rate in PEMFC
ζ	zeta potential
μ	dynamic viscosity
ρ	density
σ	standard deviation
σ_∞	bulk electrolyte conductivity
τ	tortuosity
Ψ	porosity

* Corresponding author email: cbuie@stanford.edu

THEORY

Electroosmosis (EO) is the bulk motion of liquid caused by electrical forces acting on diffuse net charge regions of an electric double layer (EDL) that forms at an electrolyte/solid interface. Net charge available for EO pumping accumulates in the diffuse portion of the EDL. The flow rate, pressure, and efficiency of porous glass electroosmotic pumps has been modeled and well characterized [12,13]. Figure 1c shows an idealized schematic of an EO pump. The flow rate, Q , of an EO pump is

$$Q = \frac{\psi}{\tau} \left[-\frac{\Delta P A a^2}{8\mu L} - \frac{\varepsilon \zeta A V_{eff}}{\mu L} f \right], \quad [1]$$

where ψ is porosity, τ is tortuosity, ΔP is pressure drop across the pump, A is cross-sectional area of the pumping media, a is pore diameter, μ is dynamic viscosity of the fluid, ε is permittivity of the fluid, ζ is zeta potential of the fluid/solid interface, and L is pump thickness. V_{eff} is the effective potential drop across the porous structure. The parameter f takes into account the effects of finite EDLs and is determined from numerical solutions to the nonlinear Poisson-Boltzmann equation governing the electric potential, ϕ , in the channels [12]. The maximum flow rate and maximum pressure produced by an EO pump can be derived from Eq. [1]. The maximum current density that the EO pump draws is

$$I_{eo}'' = \frac{\psi \sigma_{\infty} V_{eff} f}{\tau L g}, \quad [2]$$

The variable g is a function of the electric potential distribution in the pore, effective electrolyte cation and anion molar conductivities, bulk conductivity of the electrolyte, σ_{∞} , and the Debye length of the solution [12]. The maximum power consumed by the EO pump can be expressed as

$$P_{eo}'' = V_{app} I_{eo}'', \quad [3]$$

where V_{app} is the total potential applied to the pump, related to V_{eff} as

$$V_{eff} = V_{app} - V_{dec} - 2R_A I_{eo}'', \quad [4]$$

Here V_{dec} is the decomposition potential (including theoretical electrode potentials and overpotential) associated with Faradaic electrode reactions. R_A is the electrode-to-pump structure electric resistance. Together, Equations 1 through 4 provide a model for the power consumed by an EO pump.

Next, we present simple relations for fuel cell water production and power generation. The stoichiometric volume flow rate of air required by a fuel cell can be expressed as a function of the fuel cell current, I_{fc} , generated as

$$Q_{air,stoich} = \frac{R_u T}{4F} \frac{I_{fc}}{p_{air} s}, \quad [5]$$

where R_u is the universal gas constant, F is Faraday's constant, $s = 0.21$ is the volume fraction of oxygen in air, p_{air} is the pressure of the air, and T is temperature. The ratio of the volume flow rate of air entering the fuel cell to that of produced water is

$$\beta = \frac{Q_w}{Q_{air,stoich}} = 2s \frac{M_w \rho_a}{M_a \rho_w}, \quad [6]$$

where M is the molecular weight and ρ is the density for subscripts a (air) and w (water). For illustrative purposes we will assume that all water produced is in liquid form; then ρ_w is 1000 kg/m³ and β is 22.5E-5. A 1 cm² fuel cell (similar to the

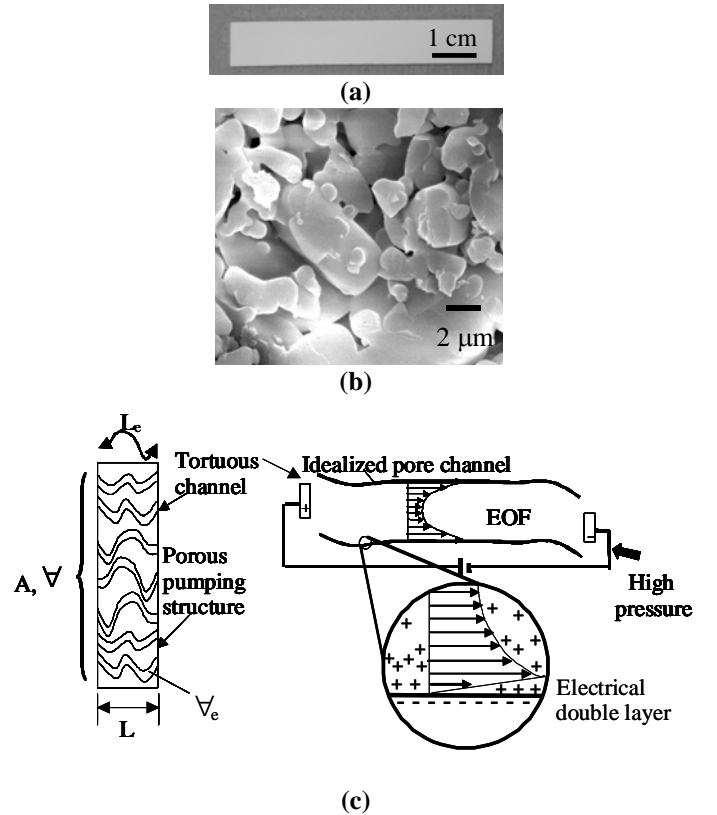


Figure 1: Porous glass electroosmotic pumps (EOPs). (a) Image of a 1 by 6 cm porous glass frit used here. (b) A scanning electron micrograph of porous glass frit structure. EOPs are modeled as a series of tortuous microchannels in parallel (c). Electrolyte/wall interfaces spontaneously form electric double layers (EDLs). Pumping structure is characterized by cross sectional area, A , volume, V , void volume, V_e , length L , and the tortuous characteristic length of pores L_e . The ratios V_e/V and $(L_e/L)^2$ are porosity and tortuosity, respectively.

fuel cells used in this study) can generate 1 A of current at

0.5 V, producing 500 mW of power. Using Eq. [6], 4 $\mu\text{L}/\text{min}$ of liquid water should be produced at the cathode under these conditions. This does not account for water transported from the anode to the cathode by electroosmotic drag or water produced in vapor form. Given this flowrate of water, an EOP would theoretically consume 25 mW of power. The primary characteristics of this pump are summarized in Table 1. The values for ζ , f , g , and σ_∞ are consistent with deionized water exposed to the atmosphere (i.e., saturated with carbon dioxide from the room) at 70°C. This simple model suggest that EO pumps can be used to remove adequate flow rates of water from fuel cells with a relatively small amount of the power produced by the fuel cell.

A	12 cm^2
L	1.1 mm
ζ	80.8 mV
σ_∞	3E-04 S/m
a (radius)	0.5 mm
ψ	0.28
τ	1.45
V_{app}	13 V
V_{eff}	10 V
f	0.97
g	0.66

Table 1: Parameters used in EO pump power calculation.

EXPERIMENTAL METHODOLOGY

The purpose of this experimental study is to evaluate the benefit of integrating electroosmotic pumps with PEMFCs. For this reason, the design of the fuel cell is limited to a single, linear cathode air channel. Prior research on cathode flooding has been performed on similar cells [4] and this design was chosen in order to decrease the number of experimental variables and enable controlled experiments. The fuel cell design is shown in Figure 2. The anode current collector is a

1mm thick stainless steel plate with a wire electrical discharge machined (EDM-Tek, Union City, CA) 2 by 60 mm flow channel for hydrogen. The plate has an evaporated gold layer roughly 1 μm thick. The membrane electrode assembly (MEA) (BCS Fuel Cells Inc. Bryan, TX) consists of a 51 μm thick Nafion membrane (Nafion 112) with 350 μm thick carbon cloth gas diffusion layers (GDLs) and a 1 mg/cm^2 platinum catalyst loading. The dimensions of the GDL are 6 mm width and 66 mm in length. The current collector on the cathode side of the fuel cell is a solid Pt mesh (Goodfellow Cambridge Limited) which also serves as the anode of the electroosmotic pump. Platinum is used for corrosion resistance; and we are currently evaluating devices with less expensive substrates, including steel with a sputtered platinum coating. The platinum mesh shown above the electroosmotic pump in the schematic is the EO pump cathode electrode. Water that forms in the fuel cell cathode channel wicks into the porous frit structure via capillary action. A sufficient amount of water in the frit completes the electrolytic circuit of the EO pump. When a potential is applied to the pump, water is pumped out of the cathode air channels and into the reservoirs located in the acrylic top plate. This water can be collected here or purged out of the device. The fuel cell cathode doubles as the anode of the EO pump.

The experiments outlined in this work were performed at the Stanford Microfluidics Laboratory with strong support from the Stanford Rapid Prototyping Laboratory. The experimental setup consists of a fuel cell, a power supply (Acopian W3.3MT65, Easton, PA) set at 3.3 V, and an electronic load (Agilent N3100A). The power supply is connected in series with the fuel cell to supplement the voltage provided by the electronic load. The load is operated in a four-wire mode with the source wires connected to the series combination of the fuel cell and the boost power supply, and the sense wires connected to the fuel cell. The air and hydrogen flow rates are controlled using two Alicat Scientific 16 Series mass flow controllers (Tucson, AZ) calibrated for air and hydrogen, respectively.

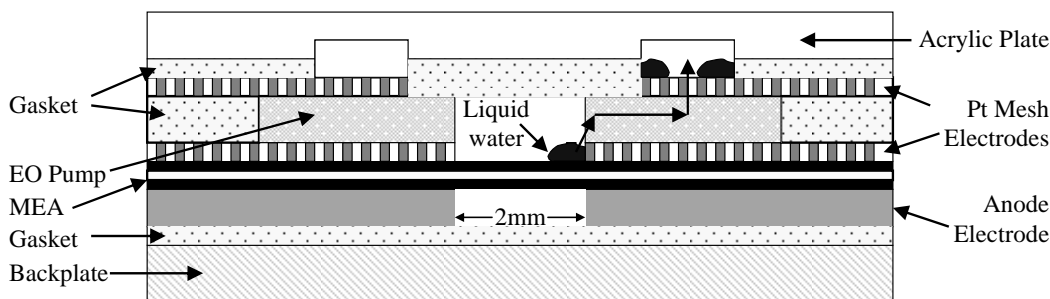


Figure 2: Schematic of the cross-sectional area of our PEMFC design showing integrated electroosmotic pumping structures. Hydrogen and air flows into the page. Water formed due to oxygen reduction at the cathode is forced out of the hydrophobic GDL where it coalesces into droplets. Liquid water droplets are wicked into the hydrophilic porous glass structure of the EO pump, and are then pumped into reservoirs integrated into the acrylic top plate.

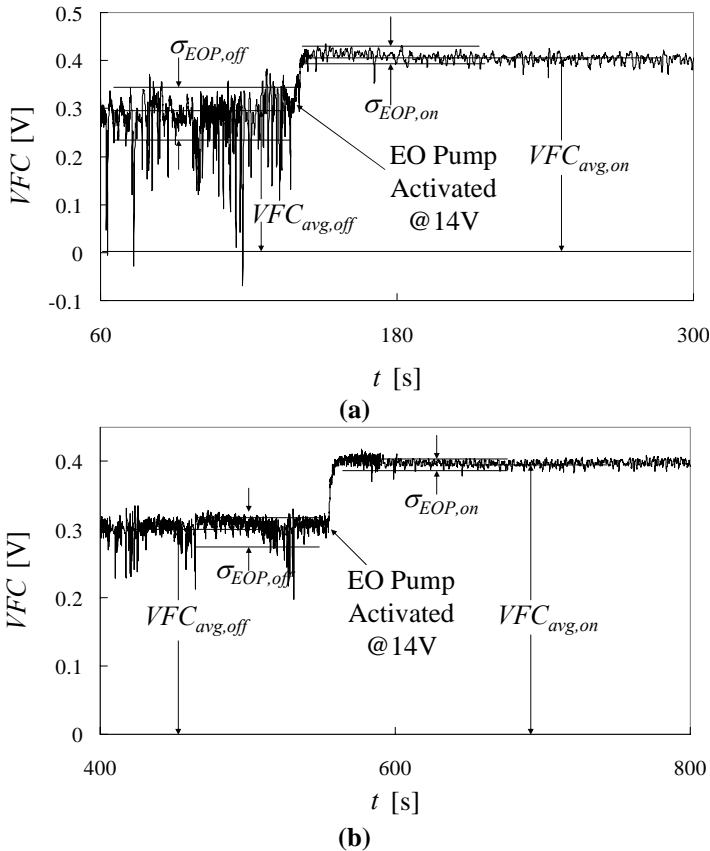


Figure 3: Galvanostatic (fixed current) measurements versus time. Experiments performed at a current density of 1 A/cm^2 with $\alpha = 2$ (a) and $\alpha = 3$ (b). Activation of EO pumps clearly benefit the flooded fuel cell and increase voltage by 120 mV and 90 mV, respectively, for $\alpha = 2$ and $\alpha = 3$. Standard deviation, σ , and average fuel cell voltage, $V_{FC,avg}$, are used to summarize the advantages of water removal using EO pumps.

The Agilent load is controlled via GPIB, and the Alicat mass flow controllers are integrated with LabView 7 using a National Instruments PCI-6031E DAQ card with an SCB-100 breakout unit. The power for the electroosmotic pump is supplied by an Agilent 6030A DC power supply. Air and hydrogen are supplied to the system from compressed gas cylinders located in the vicinity of the experimental setup. The gases exiting the flow controllers are humidified using a sparging unit with a water bath at 60°C .

Preliminary experiments demonstrated that, without activation of the EO pump, our fuel cell floods across a wide range of conditions. For example, with the active load set at 1.2 A and $\alpha = 2$, fuel cell output voltage decreased to less than 0.25 V (indicating flooding) within about 40 min. Since the time it takes to flood varies significantly with α and current density, we employed an active flooding process to expedite experiments and achieve repeatable flooding. Before each experiment, we injected water into the cathode flow channel. The majority of this water is blown out of the cathode channels at the start of the experiment as air flow rate increased to the

specified value. Liquid water that remains in the channel floods the cathode of the fuel cell (e.g., by covering portions of the GDL and inhibiting oxygen transport [4]). We refer to this situation as externally-induced flooding.

RESULTS

Figure 3 shows representative results of output voltage for fuel cells that were initially externally flooded. In each case the data is characterized by a relatively low absolute value and high standard deviation of the PEMFC potential for the case of an inactive EO pump. Upon activation of the EO pump, the PEMFC potential repeatedly and significantly rises within 5-10 s. The potential applied to the EO pump is approximately

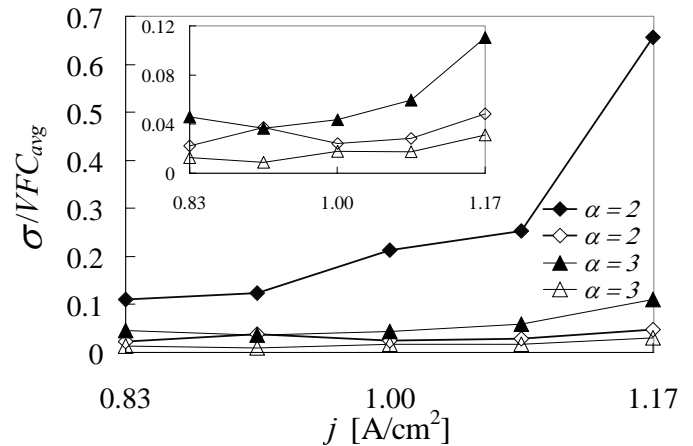


Figure 4: Normalized standard deviation of fuel cell potential versus current density, j , for $\alpha = 2$ and $\alpha = 3$. Open symbols represent cases with an activated EO pump; closed symbols indicate a deactivated EO pump. The normalized standard deviation of the fuel cell voltage with an inactive EO pump is at least twice the value of the cell with an activated pump.

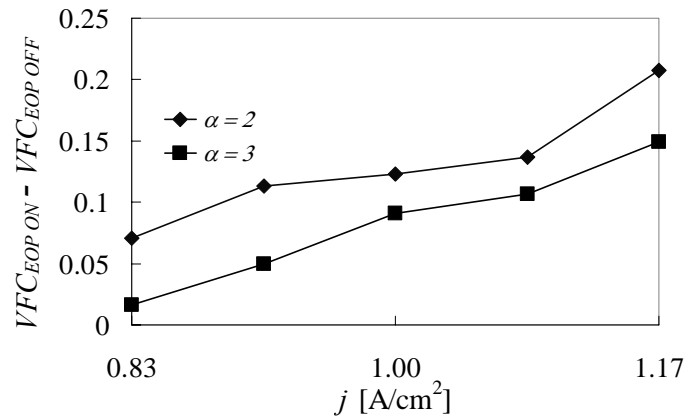


Figure 5: Difference between average fuel cell potential with activated and deactivated EO pumps as a function of current density. The benefit of EOP water removal increases with current density. This preliminary data suggests that the effect of EO pump water removal is greatest at lower α and higher j .

14 V and the pump current is 4 mA; resulting in power consumption of 56 mW. In the experiment shown in Figure 3a, the fuel cell power with the EO pump deactivated is 336 mW. This total output power increases to 480 mW upon activation of the EO pump, an increase of 144 mW. The parasitic power of the EO pump is 12% of the fuel cell power. Our preliminary experiments suggest that this parasitic power can be substantially reduced by implementing pulsed modulation of the potential to the EO pump, and we are currently pursuing such control schemes. We are also evaluating voltage conversion schemes to directly power the EO pump with fuel cell power.

In Figures 4 and 5, fuel cell output performance is compared for the cases where the EO pump is activated or deactivated. Stoichiometric ratios of air flow rate, α , of 2 and 3 are shown and fuel cell current densities range from 0.83 A/cm² to 1.17 A/cm². The case of lower α has negligible advection of water from air channels and suffers from continued and more rapid flooding. This flooding condition benefits strongly from EO pumping of liquid water. Figures 4 and 5 also suggest that the benefit of EO pumping is greater for higher fuel cell current density. Higher current densities produce more liquid water and again favor flooding. In addition to reduced cell potential, we also attribute strong signal fluctuations to flooding [9,14]. Figure 4 shows that the EO pump significantly reduces fluctuations in cell potential, particularly for the $\alpha = 2$ case.

SUMMARY

We have designed and tested a single channel PEMFC with integrated EO pumps for removal of water. We have conducted experiments showing that the PEMFC benefits from an integrated EO pump device, particularly at lower α and higher current densities. Future work will consist of further characterization of PEMFC performance with integrated EO pumps using more detailed fuel cell diagnostics such as measurements of polarization curves, electrochemical impedance spectroscopy (EIS) and a segmented electrode design. Further studies are also under way on more practical fuel cell designs with larger active areas and more complex cathode flow channel structures.

ACKNOWLEDGMENTS

C.R. Buie is funded by a National Science Foundation Graduate Research Fellowship.

REFERENCES

[1] Larminie, J., Dicks, A., 2003, *Fuel cell systems explained*; Wiley.

[2] Lee, S.J., Chang-Chien, A., Cha, S.W., O'Hayre, R. Park, Y.I., Saito, Y., Prinz, F.B., 2002, "Design and fabrication of a micro fuel cell array with "flip-flop" interconnection," *Journal of Power Sources*, 112 (2), pp. 410-418.

[3] Baschuk, J.J., Li, X., 2000, "Modeling of polymer electrolyte membrane fuel cells with variable degrees of water flooding," *Journal of Power Sources*, 86 (1-2), pp. 181-196.

[4] Tuber, K., Pocaza, D., Hebling, C., 2003, "Visualization of water build up in the cathode of a transparent PEM fuel cell," *Journal of Power Sources*, 124 (2), pp. 403-414

[5] He, W., Yi, J.S., Nguyen, T.V., 2000, "Two-phase flow model of the cathode of PEM fuel cells using interdigitated flow fields," *AIChE Journal*, 46 (10), pp. 2053-2064 .

[6] Itonen, J., Mikkola, M., Lindbergh, G., 2004, "Flooding of gas diffusion backing in PEFCs: Physical and Electrochemical characterization" *Journal of the Electrochemical Society*, 151 (8), pp. A1152-A1161.

[7] He, W., Nguyen, T.V., 2004 "Edge effects on reference electrode measurements in PEM fuel cells," *Journal of the Electrochemical Society*, 151 (2), pp. A185-A195.

[8] Satija, R., Jacobson, D.L., Arif, M., Werner, S.A., 2004, "In situ neutron imaging technique for evaluation of water management systems in operating PEM fuel cells," *Journal of Power Sources*, 129 (2), pp. 238-245.

[9] Ge, S., Li, X., Hsing, I.M., 2005, "Internally humidified polymer electrolyte fuel cells using water absorbing sponge," *Electrochimica Acta*, 50, pp. 1909-1916.

[10] Nguyen, T.V., Knobbe, M.K., 2003, "A liquid water management strategy for PEM fuel cell stacks," *Journal of Power Sources*, 114 (1), pp. 70-79.

[11] Knobbe, M.W., He, W., Chong, P.Y., Nguyen, T.V., 2004, "Active gas management for PEM fuel cell stacks," *Journal of Power Sources*, 138 (1-2), pp. 94-100.

[12] Yao, S., Santiago, J.G., 2003, "Porous glass Electroosmotic pumps: theory," *Journal of Colloid and Interface Science*, 268, pp. 133-142.

[13] Yao, S., Hertzog, D.E., Zeng, S., Mikkelsen, J.C., Santiago, J.G., 2003, "Porous glass Electroosmotic pumps: design and experiments," *Journal of Colloid and Interface Science*, 268, pp. 143-153.

[14] Barbir, F., Gorgun, H., Wang, X., 2005, "Relationship between pressure drop and cell resistance as a diagnostic tool for PEM fuel cells," *Journal of Power Sources*, 141 (1), pp. 96-101.